Periodica Polytechnica
Mechanical Engineering

58(1), pp. 27-35, 2014
DOI:10.3311/PPme.7381

Research on the Piston with Damping Hole and Pressure Recess of Axial Piston Motor

Z-Q Wang, L-Y Gu, J-W Cheng, Y-Y Wang, M Gao, X-J Jia

RESEARCH ARTICLE

RECEIVED 23 SEPTEMBER 2013; ACCEPTED 28 JANUARY 2014

Abstract

Based on the principle of hydrostatic bearing, in this study, several novel kinds of pistons were designed out, and the mathematic model of hydrostatic bearing on piston was established and analyzed. It was also found that, the diameter of damping hole and the width of pressure recess had impact on the radial load capacity of piston, the overall efficiency of axial piston motor, and the friction and wear capacity of piston. Results from tests shown that in the case of the pressure difference of 10MPa to 22MPa and the different speed of 500rpm to 2000rpm, the overall efficiency of axial piston motor could be improved by 0.1%-0.6%, compared to the ordinary piston. On the other hand, the wear scar of the piston modified was circular, and the one of the ordinary piston was longitudinal and deep, which shown that the piston modified could improve the wear capacity.

Keywords

axial piston motor · hydrostatic bearing · damping hole · efficiency · friction

Z-Q Wang
The State Key Laboratory of Fluid Power Transmission and Control, Zhejiang University, Hangzhou, Zhejiang, 310027, China
e-mail: wangzhaoqiang_2008@126.com
L-Y Gu
J-W Cheng
Y-Y Wang
M Gao
X-J Jia
The State Key Laboratory of Fluid Power Transmission and Control, Zhejiang University, Hangzhou, China

1 Introduction

A substantial portion of research today is concentrated on energy savings. In relation to the consumption of energy, efficiency inevitably becomes a priority. It is thus necessary to reduce friction and to decrease wear so as to improve machines' performances and to minimize energy losses. In the recent years, there are many researches on the friction between piston and cylinder boring. Kumar, S. and Bergama, J. M. clarified the effect of grooves cut along the pistons surface via studying the effect of the number of grooves and their location over the piston surface [1]. The piston attained different eccentricity positions during a stroke. The eccentricity of the piston affected the performance of the cylinder by influencing the frictional and leakage aspects [2]. The groove axial length, number and position had influence on the total side thrust acting on a spool inserted into a tapered clearance [3]. Fang, Y. and Shirakashi, M. presented a method for evaluating the lubrication characteristics between the piston and cylinder in a swash-plate type axial piston pump-motor under mixed lubrication conditions [4]. Ivantysynova, M., et al. designed a new test device, which was developed to measure dynamic pressure fields and temperature distribution in the gap between the piston and cylinder of swash plate axial piston machines [5], and established a novel thermal model for the piston/cylinder interface of piston machines [6], recently it was presented that waviness of the solid bodies actually reduced the power loss and improved lubrication on the fluid film surfaces of piston [7].

Wang, X. and Yamaguchi, A. had discussed that the load-carrying capacity, power losses and stiffness of disk-type hydrostatic thrust bearings including the case of eccentric loading. The power loss due to leakage was slightly larger, but power loss due to friction was much smaller than in the case of hydraulic oil, which is in contrast to the study in the paper [8]. A numerical study concerning the performance of non-recessed hole-entry hybrid journal bearing lubricated with micro polar lubricants was presented [9]. A hydrostatic bearing was described whereby the oil pockets and capillary feeds were incorporated in a stationary central shaft to support an

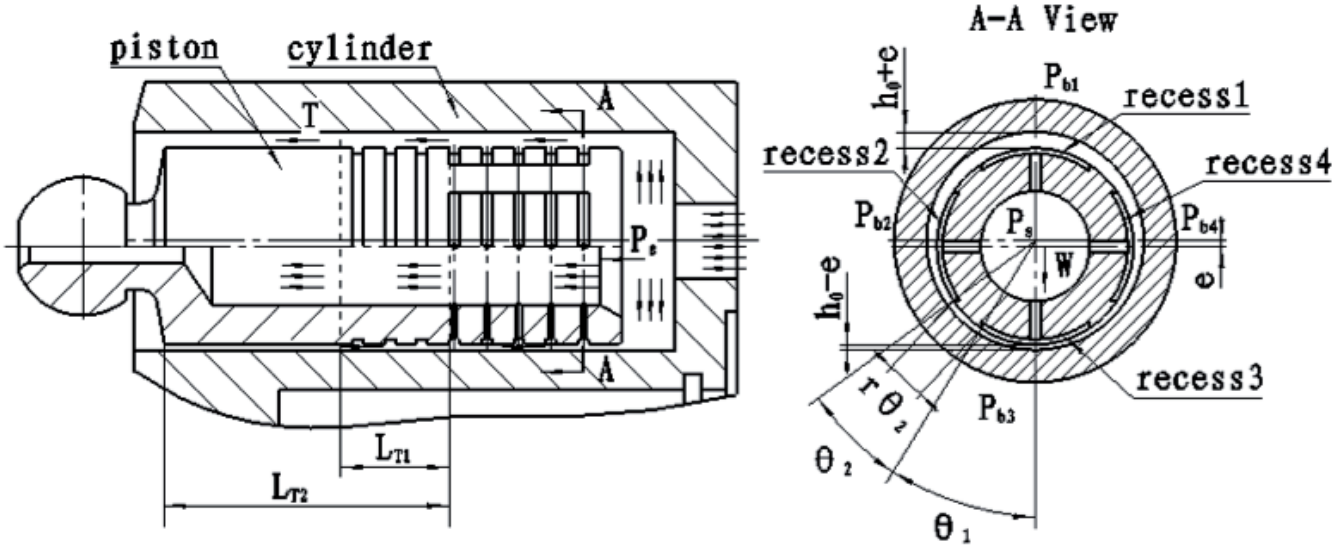

Fig. 1. Schematic of a four-recess hydrostatic journal bearing system

external rotor [10]. Nicodemus, ER. and Sharma, SC. studied analytically the performance of four-pocket orifice compensated hydrostatic/hybrid journal bearing system of various geometric shapes of recess operating with micro polar lubricant [11]. Performance data were developed for a four-pocket bearing. The effects of rotation and the feeding system on the stiffness, load capacity, flow and attitude angle were discussed [12]. Gabermann, M. developed an anti-stiction device called the airpel air cylinder, whose principle is similar to the study, to overcome the problem of stiction. It is a nearly frictionless air cylinder that virtually eliminates both starting and running friction using a unique combination of materials and a novel construction [13]. Belforte, G., et al. designed and developed pneumatic cylinders without mechanical seals in order to drastically reduce friction forces and allow continuous positioning by feedback control. The duct configuration by a central vent avoids any interference between chamber pressures [14]. However, so far few studies are available that focuses on the detail investigation of the piston based on the principle of hydrostatic bearing. The paper preliminarily established the mathematic model of the piston frictional pair under simplified conditions. On the other hand, five different kinds of pistons were tested under different operational conditions. The results presented in this study are expected to be quite useful for axial piston motor designers.

2 Mathematical model of hydraulic-static bearing on piston

Fig. 1 shows schematic of a four-recess hydrostatic journal bearing system. The piston is equal to the shaft. The cylinder bore is equal to the hydrostatic bearing. During a stroke, the lateral force imposes on the piston, and the piston attains different eccentricity positions. When the oil with high pressure P_s flows into the cylinder bore, and flows into the port with low

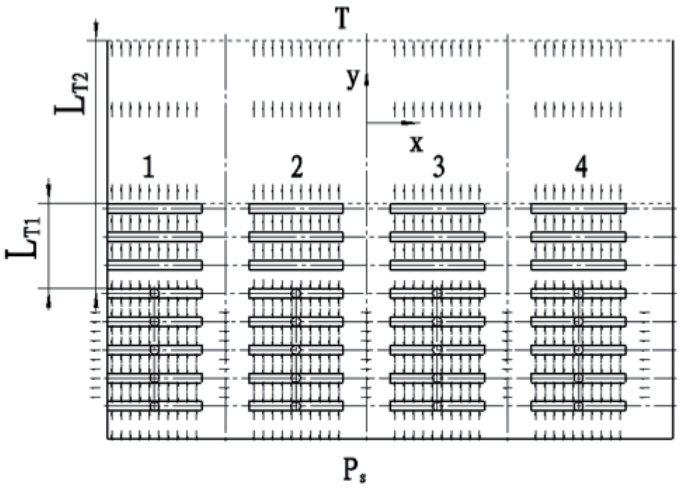

Fig. 2. Developed surface of bearing

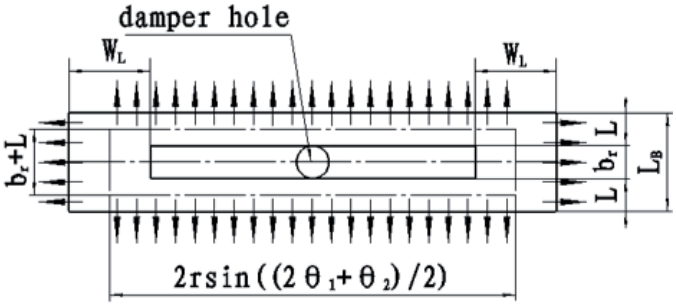

Fig. 3. Developed surface of single groove

pressure T through radial damper and circular gap. Because of lateral force imposed on the piston, the piston migrates away from the center position. The top oil film is thicker than the bottom one, so the pressure P_{b1} of the recess 1 is lower than the

one P_{b3} of recess 3. Therefore, the pressure difference between P_{b1} and P_{b3} could push the piston to the direction of the center. The inner leakage from recess 3 to recess 1 in circular direction will occur, because the pressure of recess 3 is higher than the one of recess 1(shown as in Fig. 2). The x direction is defined as the axial direction, and the y direction is defined as the circumferential direction.

Just as shown in Fig. 3, it is the developed surface of single recess, the top row of hydrostatic bearing primarily imposes effect, because there is no axial oil flow for these rows except from the top one. Here the top row of hydrostatic bearing is only calculated.

3 Hydrostatic bearing leakage

Here it is assumed that the piston will move only parallel to cylinder boring, and the dimension tolerances are omitted.

3.1 Leakage between piston and cylinder bore

The flow rate from circular gap between the piston and cylinder bore shown in Fig. 2.

$$Q_{T1} = \frac{\pi d h_0^3 P_s}{12\mu L_{T1}} \tag{1}$$

$$Q_{T2} = \frac{\pi d h_0^3 P_s}{12\mu L_{T2}} \tag{2}$$

$$Q_{avg} = \frac{Q_{T1} + Q_{T1}}{2} \tag{3}$$

$$P_{avg} = Q_{avg} \times P_s \tag{4}$$

The flow rate from circular gap between the piston and cylinder bore shown in Fig. 4.

$$Q'_{T1} = \frac{\pi d h_0^3 P_s}{12\mu L'_{T1}} \tag{5}$$

$$Q'_{T2} = \frac{\pi d h_0^3 P_s}{12\mu L'_{T2}} \tag{6}$$

$$Q'_{avg} = \frac{Q'_{T1} + Q'_{T2}}{2} \tag{7}$$

$$P'_{avg} = Q'_{avg} \times P_s \tag{8}$$

Where $L_{T1} < L'_{T1}$, $L_{T2} < L'_{T1}$, it can be gotten that $P_{avg} > P'_{avg}$.

The additional power loss resulted from leakage compared to the unmodified structure

$$P_L = P_{avg} - P'_{avg} \tag{9}$$

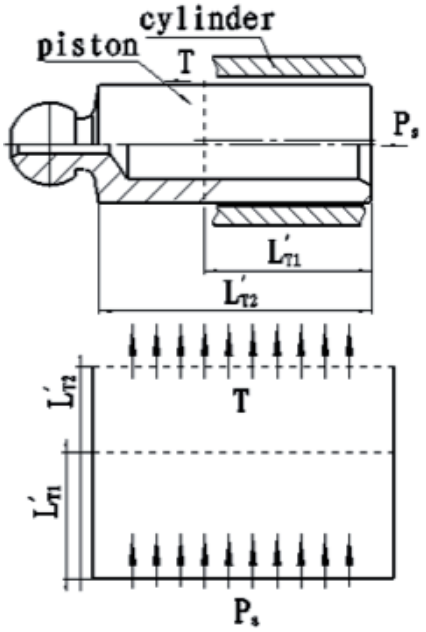

Fig. 4. Schematic of leakage on piston-cylinder system

3.2 Load capacity model of hydrostatic bearing

The projection area A_b of single recess

$$A_b = 2r\left(b_r + L\right)\sin\left(\frac{\pi}{4}\right) \tag{10}$$

The flow rate pasts through the damper

$$Q'_{b0} = C_d \frac{\pi d_0^4}{4}\sqrt{\frac{2\left(P_s - P_{b0}\right)}{\rho}} \tag{11}$$

The flow rate Q_{b0} of oil flows out from a recess.

It is assumed that the oil only flows out in axial direction.

$$Q_{b0} = \frac{\pi r h_0^3 P_{b0}}{12\mu L} \tag{12}$$

The pressure is equal in all the recesses without load. The flow rate Q_{b0} of oil which flows out from a recess is equal to the one which pasts through the damper.

$$Q'_{b0} = Q_{b0} \tag{13}$$

Substituted the Eq. (12) and Eq. (13) into Eq. (14), then

$$C_d \frac{\pi d_0^2}{4}\sqrt{\frac{2\left(P_s - P_{b0}\right)}{\rho}} = \frac{\pi r h_0^3 P_{b0}}{12\mu L} \tag{14}$$

From Eq. (14), the parameter of structure can be derived as.

$$\lambda_0 = \frac{P_s - P_{b0}}{P_{b0}} = \frac{\rho r^2 h_0^6}{18 C_d^2 d_0^4 \mu L} P_{b0} \tag{15}$$

The pressure ratio of λ_k

$$\lambda_k = \frac{P_s}{P_{b0}} \tag{16}$$

The load capacity W of hydrostatic bearing

$$W = A_b\left(P_{b3} - P_{b1}\right) \tag{17}$$

The piston will migrate away from the center position under the load, so the oil film thickness of recess 1 and recess 3 will change.

$$h_1 = h_0\left(1+\varepsilon cos\theta_1\right) \tag{18}$$

$$h_3 = h_0\left(1-\varepsilon cos\theta_1\right) \tag{19}$$

The oil film thickness of recess 2 and recess 4 are equal, then

$$h_2 = h_4 = h_0 \tag{20}$$

That is to say

$$P_{b2} = P_{b4} = P_{b0} \tag{21}$$

Under the load condition of the piston, the flow rate is divided into the axial and circumferential flow rate.

$$Q_{Axial} = \frac{\pi r h_0^3\left(1-\varepsilon cos\theta_1\right)^3}{12\mu L} P_{b3} \tag{22}$$

$$Q_{Inner} = \frac{b_r h_0^3\left(P_{b3} - P_{b1}\right)}{12\mu\theta_2} \tag{23}$$

According to the flow continuity equation, then

$$Q'_{b0} = Q_{Axial} + Q_{Inner} \tag{24}$$

Substituted Eqs. (11), (22) and (23) into Eq.(24)

$$\begin{aligned} &C_d\frac{\pi d_0^2}{4}\sqrt{\frac{2\left(P_s - P_{b3}\right)}{\rho}} \\ &= \frac{\pi r h_0^3\left(1-\varepsilon cos\theta_1\right)^3}{12\mu L} P_{b3} + \frac{b_r h_0^3\left(P_{b3} - P_{b1}\right)}{12r\theta_2} \end{aligned} \tag{25}$$

$$\frac{W}{A_b} = P_{b3} - P_{b1} \tag{26}$$

Then

$$\begin{aligned} &\frac{C_d^2\pi^2 d_0^4}{8\rho} P_s - \frac{C_d^2\pi^2 d_0^4}{8\rho} P_{b3} \\ &= \frac{\pi^2 r^2 h_0^6\left(1-\varepsilon cos\theta_1\right)^6}{144\mu^2 L^2} P_{b3}^2 \\ &+ \frac{\pi h_0^6 W\left(1-\varepsilon cos\theta_1\right)^6 b_r}{72\mu L\theta_2 A_b} P_{b3} + \frac{b_r^2 h_0^6 W^2}{144 r^2\theta_2^2 A_b^2} \end{aligned} \tag{27}$$

Defined as

$$a_1 = \frac{\pi^2 r^2 h_0^6\left(1-\varepsilon cos\theta_1\right)^6}{144\mu^2 L^2}$$

$$a_2 = \frac{\pi h_0^6 W\left(1-\varepsilon cos\theta_1\right)^3 b_r}{72\mu L\theta_2 A_b}$$

$$a_3 = \frac{b_r^2 h_0^6 W^2}{144 r^2\theta_2^2 A_b^2}$$

$$a_4 = \frac{C_d^2\pi^2 d_0^4}{8\rho}$$

Then

$$a_1 P_{b3}^2 + \left(a_2 + a_4\right) P_{b3} + a_3 - a_4 P_s = 0 \tag{28}$$

It can be derived from Eq. (28)

$$P_{b3} = \frac{-\left(a_2 + a_4\right) \mp \sqrt{\left(a_2 + a_4\right)^2 - 4a_1\left(a_3 - a_4 P_s\right)}}{2a_1} \tag{29}$$

Where

$$P_{b3} \geq = 0; a_1, a_2, a_3, a_4 > 0$$

Then

$$P_{b3} = \frac{-\left(a_2 + a_4\right) + \sqrt{\left(a_2 + a_4\right)^2 - 4a_1\left(a_3 - a_4 P_s\right)}}{2a_1} \tag{30}$$

The pressure of recess 1 can be gotten according to the method above

$$\begin{aligned} &C_d\frac{\pi d_0^2}{4}\sqrt{\frac{2\left(P_s - P_{b1}\right)}{\rho}} \\ &= \frac{\pi r h_0^3\left(1+\varepsilon cos\theta_1\right)^3}{12\mu L} P_{b1} - \frac{b_r h_0^3\left(P_{b3} - P_{b1}\right)}{12r\theta_2} \end{aligned} \tag{31}$$

Defined as

$$a_5 = \frac{\pi^2 r^2 h_0^6 \left(1+\varepsilon cos\theta_1\right)^6}{144\mu^2 L^2}$$

$$a_6 = \frac{\pi h_0^6 W \left(1+\varepsilon cos\theta_1\right)^3 b_r}{72\mu L\theta_2 A_b}$$

Then

$$P_{b1} = \frac{-\left(a_4-a_6\right)+\sqrt{\left(a_4-a_6\right)^2-4a_5\left(a_3-a_4P_s\right)}}{2a_5} \quad (32)$$

Substituted Eqs. (30) and (32) into Eq. (17), then

$$\begin{aligned} W &= A_b\left(p_{b3}-p_{b1}\right) \\ &= A_b\left[\frac{-\left(a_2+a_4\right)+\sqrt{\left(a_2+a_4\right)^2-4a_1\left(a_3-a_4P_s\right)}}{2a_1}\right. \\ &\quad \left.-\frac{-\left(a_4-a_6\right)+\sqrt{\left(a_4-a_6\right)^2-4a_5\left(a_3-a_4P_s\right)}}{2a_5}\right] \\ &= 12A_b p_s \varepsilon cos\theta_1 \frac{\lambda_0}{\left(1+\lambda_0\right)\left(1+2\lambda_0\right)+2\lambda_k\lambda_0\left(\lambda_0+1\right)} \end{aligned} \quad (33)$$

The friction force can be derived as

$$F_f = W \times \xi \quad (34)$$

The power loss resulted from friction

$$P_f = F_f \times v \quad (35)$$

The velocity of piston

$$v = \omega R tan\left(\gamma\right) sin\left(\varphi\right) \quad (36)$$

The power loss improvement for single piston

$$P_{sav} = P_f - P_L \quad (37)$$

It is obvious: $p_f >> p_L$, the power loss due to friction is much larger than the one due to leakage in the case of hydraulic oil [8]. So the efficiency improvement of axial piston motor

$$\eta = NZ\frac{P_{sav}}{P_a} \approx NZ\frac{P_f}{P_a} \quad (38)$$

The input power of axial piston motor

$$P_a = \frac{P_s nV}{612} \quad (39)$$

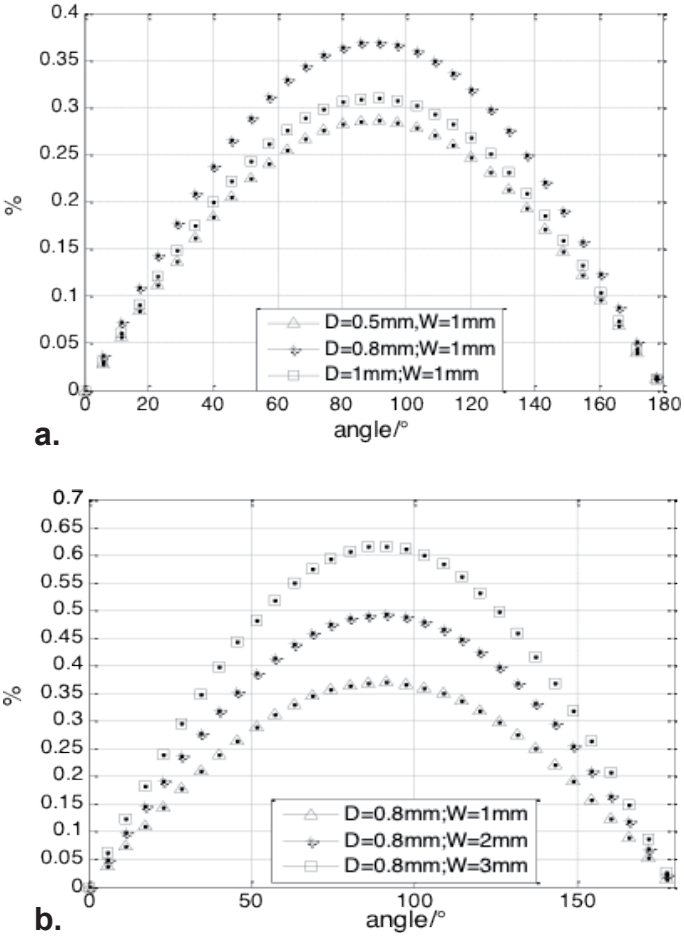

Fig. 5. Variation of efficiency improvement percentage with cylinder angle

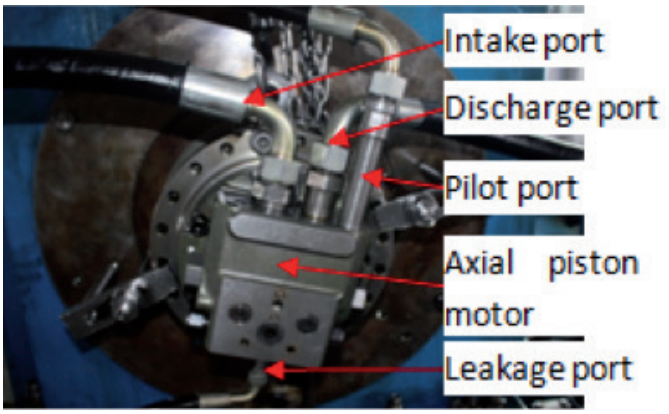

Fig. 6. Test of overall efficiency for axial piston motor on test rig

Then

$$\eta = NZ\frac{2400A_b\varepsilon cos\left(\theta_1\right)\lambda_0\xi\pi R tan\left(\gamma\right) sin\left(\varphi\right)}{V\left[\left(1+\lambda_0\right)\left(1+2\lambda_0\right)+2\lambda_k\lambda_0\left(\lambda_0+1\right)\right]} \times 100 \quad (40)$$

The relative parameters can be substituted, Fig. 5a and Fig. 5b can be gotten.

From Fig. 5a, when the recess width is 1 mm, under different diameters of damping hole 0.5 mm, 0.8 mm, 1 mm, the

efficiency improvement percentage will change following sine curve with the rotatory angle of cylinder.

From Fig. 5b, for the case of the diameter of damping hole 0.8 mm and different recess width 1 mm, 2 mm, 3 mm, the efficiency improvement percentage will change following sine curve with the rotatory angle of cylinder.

The variation of recess width has more effect on the efficiency improvement percentage compared to the variation of damping hole diameter. During the rotation of cylinder, the efficiency improvement percentage is variable.

4 Test of verification

4.1 Efficiency test

Fig. 6 shows the test rig of axial piston motor, the motor has two stage speeds, so the pilot port can rotate the swash plate in order to change the displacement. When adjusting a certain operation, writing the results of test such as pressure, flow, torque, speed. The capabilities of the bench are a maximum shaft speed of 3500 rpm, a maximum supply pressure of 35 MPa, a maximum load torque of 500 N·m and a maximum supply flow rate of 150 L/min. In order to ensure a high level of repeatability, the tests are repeated at least three times during the course of operation. All tests have been carried out using ISO VG32 mineral oil, which is used to supply the test bench. Because the circumference temperature is 30 degree, and the temperature of oil can rise up to 65 degree, the oil with low viscosity is adapted. The uncertainty levels of the measurement devices on the test rig are given in Table 1.

Fig. 7 shows the picture of pistons based on the principle of hydrostatic bearing, inside the recess the damper is drilled, Brazing the block between the two dampers. The tested pistons are made of 38 CrMnAl steel, which is carburized, case hardened, tempered and Maag criss-cross ground. The surface hardness is HRC = 56 ± 2 and the case hardness depth (CHD) is 0.6 to 0.9 mm (Eht).

Fig. 8 illustrates variation of overall efficiency of axial piston motor with velocity under different diameters. When the diameter of the damper is 0.8 mm, the overall efficiency of axial piston motor is highest among all the specimens; at the case of the diameter of the damper 0.5 mm, the overall efficiency of axial piston motor lists the second one among all the specimens; the overall efficiency of axial piston motor fixed the original piston is lowest among all the specimens; and with the increase of the rotation rate, the overall efficiency of axial piston motor decreases.

Fig. 9 illustrates variation of overall efficiency of axial piston motor with pressure under different diameters .When the diameter of the damper is 0.8 mm, the overall efficiency of axial piston motor is highest among all the specimens; at the case of diameter of the damper 0.5 mm, the overall efficiency of axial piston motor lists the second one among all the specimens; the overall efficiency of axial piston motor fixed original piston is lowest among all the specimens; and with the increase of pressure, the overall efficiency of axial piston motor increases.

Tab. 1. Measurements uncertainties

Measurement	Uncertainty
Speed	0.5%
Pressure	0.5%
Torque	0.5%
Power	0.5%
Flow	0.5%

Fig. 7. Hydrostatic bearing piston

For a certain value of supply pressure and damper diameter, the decreasing of the bearing hydraulic resistance is due to the increasing of damper diameter.

Fig. 10 illustrates variation of overall efficiency of axial piston motor with velocity under different width. When the width of the recess is 1 mm, the overall efficiency of axial piston motor is highest among all the specimens; at the case of the width of the recess 3 mm, the overall efficiency of axial piston motor lists the second one among all the specimens; the overall efficiency of axial piston motor fixed the original piston is lowest among all the specimens; and with the increase of velocity, the overall efficiency of axial piston motor decreases.

Fig. 11 illustrates variation of overall efficiency of axial piston motor with pressure under different width. When the width of the recess is 1mm, the overall efficiency of axial piston motor is highest among all the specimens; at the case of the width of the recess 3 mm, the overall efficiency of axial piston motor lists the second one among all the specimens; the overall efficiency of axial piston motor fixed the piston is lowest among all the specimens; and with the increase of pressure, the overall efficiency of axial piston motor increases. For a certain value of supply pressure and damper diameter, although the load capacity in theory increases with the increasing of recess width, the experimental result is not in agreement with it, because of the decreasing of supporting area. As a whole, the width of recess and diameter of damper have impact on the load capacity of circular oil film on between piston and cylinder bore. The test result is nearly in agreement with the theory result.

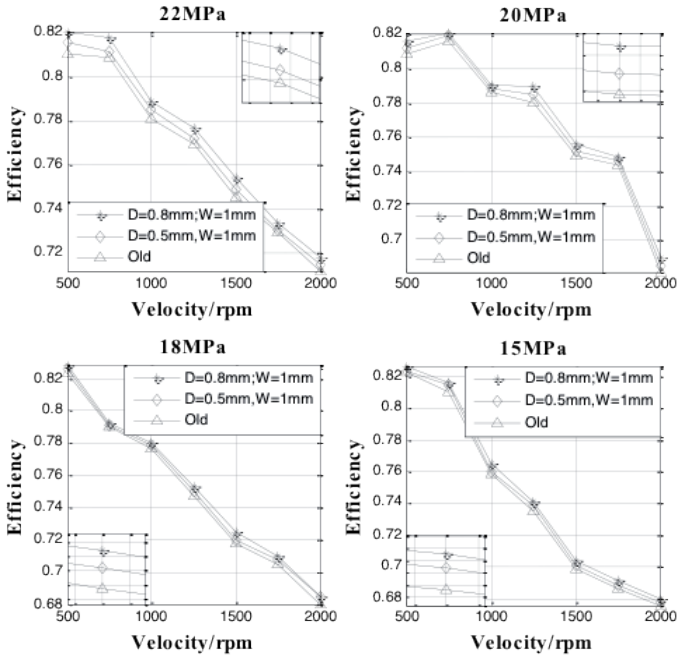

Fig. 8. Variation of overall efficiency with velocity under different diameters

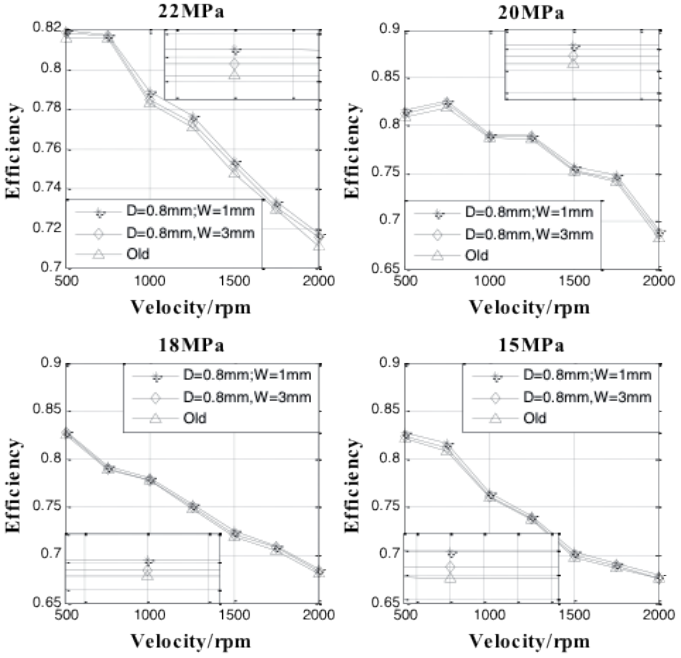

Fig. 10. Variation of overall efficiency with velocity under different width

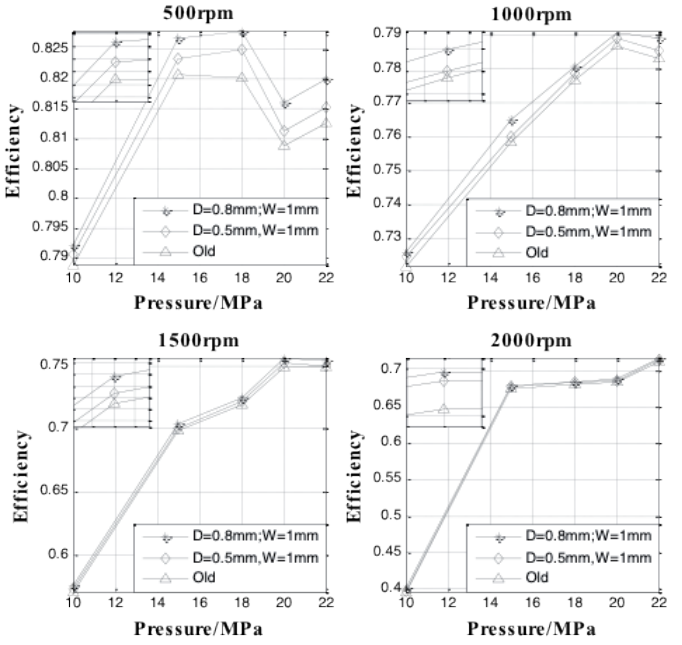

Fig. 9. Variation of overall efficiency with pressure under different diameters

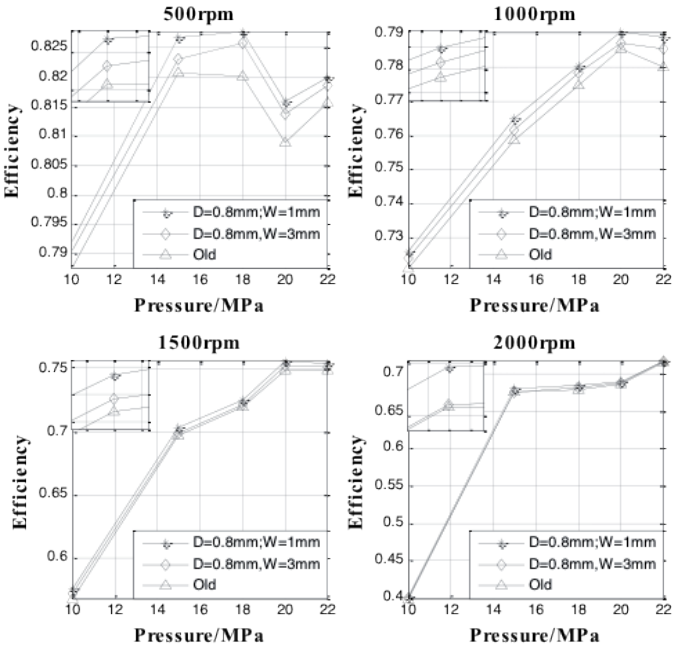

Fig. 11. Variation of overall efficiency with pressure under different width

4.2 Friction test

Just as shown in Fig. 12, it presents the comparison between normal wear pattern and modified wear pattern in the same magnification times 500 ×. The friction pattern shown in Fig. 12b, the normal wear pattern on piston without hydrostatic recess, the width of abrasion on the surface of piston are wider, there are obvious circumferential pattern. On the other hand, Fig. 12c, it is the modified wear pattern on piston with hydrostatic recess, the patterns of abrasion on the surface of piston are thin, there are no obvious circumferential pattern.

5 Conclusions

At the case of the overall efficiency of axial piston motor fixed the piston with different diameter damper. When the diameter of the damper is 0.8 mm, the overall efficiency of axial piston motor is highest among all the specimens; at the case of the diameter of the damper 0.5 mm, the overall efficiency of axial piston motor lists the second one among all the specimens; the one of axial piston motor fixed the original piston is lowest among all the specimens. The improvement of overall efficiency of axial piston motor is up to 0.25% or so.

At the case of the overall efficiency of axial piston motor fixed the piston with different width recess. When the width of the recess is 1mm, the overall efficiency of axial piston motor is highest among all the specimens; at the case of the width of the recess 3mm, the overall efficiency of axial piston motor lists the second one among all the specimens; the one of axial piston motor fixed the original piston is lowest among all the specimens. The improvement of overall efficiency of axial piston motor is up to 0.4% or so.

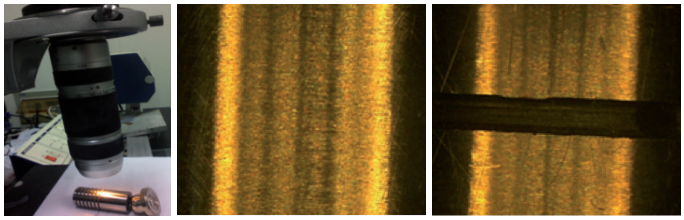

Fig. 12. Comparison between normal wear pattern and modified wear pattern (a. micro view, b. normal wear pattern, c. modified wear pattern)

As a whole, at a certain operational condition, the suitable parameters of hydrostatic bearing on the surface of the piston can produce hydrostatic force. Because the load-carrying capacity is improved, the frictional force is reduced. So the overall efficiency of axial piston motor will be improved largely, while the ability of torsion can be improved. There is the potential use of hydrostatic bearing on the piston, on the improvement of overall efficiency of axial piston motor.

Nomenclature

A_b :projection area of hydrostatic bearing, m^2
b_r :width of recess, m
C_d :flow coefficient, 0.65
d :diameter of piston, 18.2×10^{-3} m
d_0 :diameter of damper, m
e :eccentricity, m
F_f :frictional force, N
h_0 :average oil film thickness, 0.02×10^{-3} m
h_1 :oil film thickness of recess1, m
h_2 :oil film thickness of recess2, m
h_3 :oil film thickness of recess3, m
h_4 :oil film thickness of recess4, m
L :lenght of axial seal, 2×10^{-3} m
L_{T1} :shortest seal length modified, 9.1×10^{-3} m
L_{T2} :longest seal length modified, 33.75×10^{-3} m
L'_{T1} :shortest seal length unmodified, 25.1×10^{-3} m
L'_{T2} :longest seal length unmodified, 42.4×10^{-3} m
n :rotatory speed of axial piston motor, 2000 rpm
N :number of hydrostatic bearing on piston
P_a :input power of axial piston motor, w
P_{avg} :power loss modified, w
P'_{avg} :power loss unmodified, w
P_{b0} :pressure inside oil recess without load, Pa
P_{b1} :pressure of recess 1, Pa
P_{b2} :pressure of recess 2, Pa
P_{b3} :pressure of recess 3, Pa
P_{b4} :pressure of recess 4, Pa
P_f :power loss resulted from frictional force,w
P_L :power loss resulted from leakage compared to the unmodified structure,w
P_s :system pressure, Pa
P_{sav} :power conservation, w
Q_{avg} :average amount of leakage modified, m^3/s
Q_{b0} :axial leakage amount without load, m^3/s
Q_{Axial} :leakage amount of axial direction, m^3/s
Q_{Inner} :leakage amount of side direction, m^3/s
Q_{T1} :leakage of shortest seal length modified, m^3/s
Q_{T2} :leakage of longest seal length modified, m^3/s
Q'_{Avg} :average amount of leakage unmodified, m^3/s
Q'_{b0} :damper leakage amount without load, m^3/s
Q'_{T1} :leakage amount of shortest seal length unmodified, m^3/s
Q'_{T2} :leakage amount of longest seal length unmodified, m^3/s
r :radius of piston
R :radius of pitch circle located piston on cylinder, 36.5×10^{-3} m
T :tanker pressure,0Pa
W :load capacity, N
W_L :circumferential distance between two recesses on the surface of piston, m
v :velocity, m/s
V :displacement of motor, $53 \times 10^{-6}10^3$ m/r
X, Y :cartesian coordinates, m
Z :half piston number, 9

γ	:declining angle of swash plate, 0.305rad
ε	:eccentricity ratio, 0.5
η	:efficiency improvement
θ_1	:circumferential angle of recess, $\pi/6$ rad
θ_2	:circumferential angle of seal surface, $\pi/6$ rad
λ_0	:coefficient of structure
λ_k	:pressure ratio, 0.45
μ	:dynamic viscosity, 0.003728 kg · s/m^2
ξ	:frictional coefficient, 0.1
ρ	:density of oil, 898 kg/m^3
φ	:rotatory angle of cylinder, rad
ω	:angular velocity of cylinder, r/min

Acknowledgements

The authors are grateful to the Project(51004085) supported by the National Natural Science Foundation of China for the financial support and the Science Fund for Creative Research Groups of National Natural Science Foundation of China(51221004).

References

1 **Kumar S., Bergada J. M.,** *The effect of piston grooves performance in an axial piston pumps via CFD analysis*. International Journal of Mechanical Sciences, 66, 168–179 (2013). DOI: 10.1016/j.ijmecsci.2012.11.005

2 **Sadashivappa K., Singaperumal M., Narayanasamy K.,** *Piston eccentricity and friction force measurement in a hydraulic cylinder in dynamic conditions considering the form deviations on a piston*. Mechatronics, 11(3), 251–266 (2001). DOI: 10.1016/S0957-4158(00)00018-0

3 **Milani M.,** *Design hydraulic locking balancing grooves*. Proceedings of the Institution of Mechanical Engineers, Part I: Journal of Systems and Control Engineering, 215, 453-465 (2001). DOI: 10.1177/095965180121500503

4 **Fang Y., Shirakashi M.,** *Mixed lubrication characteristics between the piston and cylinder in hydraulic piston pump motor*. Journal of Tribology, 117 (1), 80–85 (1995). DOI: 10.1115/1.2830610

5 **Ivantysynova M., Huang C., Behr R.,** *Measurements of elastohydrodynamic pressure field in the gap between piston and cylinder*. in 'Power Transmission and Motion Control PTCM2005: Conference Proceedings (eds.: Johnston N., Burrows C. R., Edge K. A.)' Wiley, 451-465 (2005).

6 **Pelosi M., Ivantysynova M.,** *A Novel Thermal Model for the Piston/Cylinder Interface of Piston Machines*. in 'Proceedings of the ASME 2009 Dynamic Systems and Control Conference, Vol 2.' Paper no. DSCC2009-2782, 37-44 (2009). DOI: 10.1115/DSCC2009-2782

7 **Ivantysynova M.,** *2011 Annual Report from Maha Fluid Power research center*. Purdue University, 30 (2011).

8 **Wang, X. Yamaguchi A.,** *Characteristics of hydrostatic bearing/seal parts for water hydraulic pumps and motors, Part 2: On eccentric loading and power losses*. Tribology International, 35(7), 435–442 (2002). DOI: 10.1016/S0301-679X(02)00024-5

9 **Nathi R., Satish C.,** *Analysis of orifice compensated non-recessed hole-entry hybrid journal bearing operating with micro polar lubricants*. Tribology International, 52, 132–143 (2012). DOI: 10.1016/j.triboint.2012.03.012

10 **Martin J. K.,** *Measured stiffness and displacement coefficients of a stationary rotor hydrostatic bearing*. Tribology International, 37(10), 809-816 (2004). DOI: 10.1016/j.triboint.2004.04.010

11 **Nicodemus E. R., Sharma S. C.,** *Orifice compensated multirecess hydrostatic/hybrid journal bearing system of various geometric shapes of recess operating with micro polar lubricant*. Tribology International, 44(3), 284–296 (2011). DOI: 10.1016/j.triboint.2010.10.026

12 **Singh D. V., Sinhasan R., Ghai R. C.,** *Performance characteristics of hydrostatic journal bearings with journal rotation by a finite element method*. Wear, 45(1), 41–55 (1977). DOI: 10.1016/0043-1648(77)90101-6

13 **Gaberman M.,** *Near frictionless air cylinders provide precision pneumatic motion control system*. Power Conversion and Intelligent Motion, 11, 48-51 (1995).

14 **Belforte G., Romiti A., Raparelli T.,** *No friction cylinders for pneumatic positioners*. International Symposium on Fluid Control and Measurement, 1, 15-21 (1985).